

## EXPERIMENTAL STUDY ON FRACTURAL BEHAVIOR OF CONCRETE CONTAINING HIGH-PERFORMANCE LIGHTWEIGHT AGGREGATE

(Translation from Proceedings of JSCE, No.725/V-58, 1-13, February 2003)



Yuko ISHIKAWA



Katsuro KOKUBU



Daisuke MORI



Takahisa OKAMOTO

A recently developed high-performance lightweight aggregate offers greater strength and lower absorption than conventional artificial lightweight aggregates. The purpose of this study is to investigate the fractural behavior of lightweight concrete containing this high-performance lightweight aggregate. We carried out compressive tests and flexural fracture energy tests using acoustic emission techniques, and discovered a brittle fracture mechanism where cracks develop within aggregate particles as well as in the mortar. It was also found that improvement is obtained by enhancing the strength of the lightweight aggregate. Further tests for strength and fracture energy of concrete containing various combinations of lightweight aggregate with different qualities and a matrix with different strengths clarified the influence of aggregate quality on concrete's mechanical properties. As a result, the study as a whole represents a quantitative evaluation of variations in fracture energy with aggregate and matrix strength as well as other factors including the volume and particle size of the coarse aggregate.

**Keywords:** *high-performance artificial lightweight aggregate, lightweight concrete, fracture mechanics, fracture energy, acoustic emission*

---

Yuko Ishikawa is a deputy manager of Taiheiyo Materials Co., Ltd. Mineral & Inorganic Construction Material Sales Department, Japan. He obtained his D. Eng. from Tokyo Metropolitan University in 2001. His research interests relate to aggregates for concrete, especially lightweight aggregate. He is a member of JSCE.

---

Katsuro Kokubu is a professor in the Graduate School of Engineering at Tokyo Metropolitan University, Japan. He obtained his doctoral degree from Tokyo Metropolitan University in 1983. He is a member of concrete committee in JSCE and an administrator of JCI. His research interest includes utilization of by products as mineral admixtures, slag aggregates and recycled aggregates and compaction of concrete.

---

Daisuke Mori is a researcher of Taiheiyo Cement Co., Ltd. Research & Development Center, Japan. He obtained his M. Eng. from Chiba Institute of Technology in 1994. His research interests relate to fracture mechanics of concrete and nondestructive test of concrete structure using acoustic emission. He is a member of JSCE.

---

Takahisa Okamoto is a manager of Construction Material Business Department, in Taiheiyo Cement Co., Ltd. Japan. He obtained his Dr. of Eng. from Tokyo Institute of Technology in 1987. His research interests includes torsional and shearing behaviors of RC members, scene evaluation of concrete structures and applications of porous concrete.

---

## 1. INTRODUCTION

A lightweight concrete that enables the self weight of structures to be reduced is a material with great potential, particularly as buildings become taller, bridge spans longer, and structural cross sections larger. It would also offer advantages in a wide range of technical areas, offering reduced seismic effect, suitability for soft ground, lower lifted weight, and improved thermal insulation. However, the actual use of lightweight concretes, in civil engineering in particular, is decreasing year on year.

In fact, lightweight concrete containing conventional artificial lightweight aggregate suffers from several technical problems such as pumpability, durability, and structural performance when used in concrete members. Conventional artificial lightweight aggregate is porous and absorbs a large amount of water through the numerous open voids on its surface. Concrete with low moisture content can barely be pumped if it contains such aggregate, so the aggregate particles are usually pre-wetted before mixing. This brings the moisture content of the aggregate at the time of placing up to 20% to 30%, affecting the freeze-thaw resistance of the resulting concrete. The low strength of conventional lightweight aggregate also limits the tensile and shear strength of lightweight concrete, which renders structural members disadvantageous at the design stage. However, a recently developed artificial lightweight aggregate [1], [2] made of expanded shale (that we call here “high-performance artificial lightweight aggregate”) has much lower absorption and greater strength than the conventional material. Many studies of lightweight concrete containing this new aggregate (“high-performance lightweight concrete”) have been carried out, leading to expectations that the new aggregate will eventually overcome the problems noted above.

It has been found in previous studies [3], [4] that high-performance lightweight concrete has a drawback in its fracture characteristics. The current study was designed to obtain a systematic understanding of this issue by quantitatively evaluating the fracture characteristics of high-performance lightweight concrete containing ordinary fine aggregate and high-performance artificial lightweight coarse aggregate. Unconfined compressive and flexural fracture energy tests were carried out utilizing acoustic emission (AE) techniques to observe the fractural behavior, and further strength and fracture energy tests were carried out using concrete with various combinations of lightweight coarse aggregate quality and matrix strength and also with the content and maximum size of the coarse aggregate varied. The results were used to clarify the influence of aggregate quality on the mechanical properties of the concrete.

## 2. FRACTURE PROCESS UNDER COMPRESSIVE STRESS

### 2-1 Experiment

The behavior process exhibited by concrete as damage advances from cracking up to fracture is thought to be dependent on the occurrence, elongation, and joining-up of micro-cracks. Analysis of AE waves, or the elastic waves emitted as individual tiny fractures occur, is an effective means of investigating microscopic structural changes due to micro-cracks.

The authors measured AE waves during loading tests to determine the fractural behavior of concrete, and specifically the process whereby micro-cracks occur in high-performance lightweight concrete under unconfined compressive stress. The same test was also performed on normal concrete so that the fractural behavior of the two different types of concrete could be compared.

### 2-2 Test method

**Table 1** shows the materials used in this experiment. The high-performance artificial lightweight aggregate used was of two different densities, HL08 and HL12. Compressive strength test specimens measuring 150 mm dia. × 300 mm high were prepared in three variants following the mix proportions specified in **Table 2**: lightweight concrete specimens (LC08 and LC12) with the two different high-performance artificial lightweight coarse aggregates; and normal concrete specimens (NC). The tests were carried out using high-rigidity test equipment in accordance with the JIS A 1108 Test for Compressive Strength of Concrete. The locations indicated in **Figure 1** were fitted with 150 kHz resonant-type AE sensors to allow for AE measurements during the compression test. The AE waveform was amplified by 40 dB using a preamplifier, and signals exceeding the threshold level of 60 dB were recorded simultaneously onto six channels using an

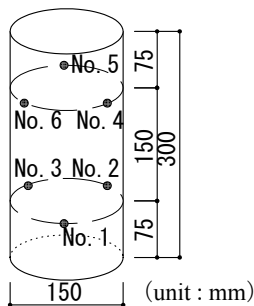
**Table 1** Materials used in concrete

Material	Symbol	Description	Properties
Cement	C	High-early-strength portland cement	Density: 3.12 g/cm <sup>3</sup> ; specific surface area: 4490 cm <sup>2</sup> /g
Fine aggregate	S	Crushed sand (Oume)	Density <sup>*1</sup> : 2.58 g/cm <sup>3</sup> ; water absorption: 1.63%; fineness modulus: 3.07
Coarse aggregate	G	Crushed stone (Oume)	Density <sup>*1</sup> : 2.62 g/cm <sup>3</sup> ; water absorption: 0.74%; maximum size: 15 mm
	HL08	High-performance lightweight aggregate	Density <sup>*1</sup> : 0.83 g/cm <sup>3</sup> ; 24-hour water absorption: 4.08%; maximum size: 15 mm
	HL12	High-performance lightweight aggregate	Density <sup>*1</sup> : 1.19 g/cm <sup>3</sup> ; 24-hour water absorption: 1.80%; maximum size: 15 mm
Chemical admixture	SP	AE superplasticizer	Main ingredient: polycarbonate ethereal composite type
	AE	AE agent	Main ingredient: modified alkylcarbonate type

\*1: oven-dry state

**Table 2** Concrete proportions

Concrete types	Symbol	Density (kg/L)	W/C (%)	s/a (%)	Air content (%)	Unit content (kg/m <sup>3</sup> )						SP (C × %)	AE (C × %)
						W	C	S	G	HL08	HL12		
Lightweight concrete	LC08	1.7	42	47.0	5.0	165	389	813	—	313	—	0.8	0.002
	LC12	1.8	42	47.0	5.0	165	389	813	—	—	421	0.8	0.002
Normal-weight concrete	NC	2.3	35	46.0	5.0	150	429	799	945	—	—	1.05	0.002

**Fig.1** Locations of AE sensors during compression testing**Table 3** Mechanical properties of concrete specimens

Symbol	Density (kg/L)	Compressive strength, $f'_c$ (N/mm <sup>2</sup> )	Tensile strength, $f_t$ (N/mm <sup>2</sup> )	Young's modulus (kN/mm <sup>2</sup> )	Modulus of brittleness ( $f'_c/f_t$ )
LC08	1.73	43.0	2.3	17.7	18.9
LC12	1.84	56.9	3.6	21.9	15.9
NC	2.38	42.5	3.5	33.3	12.2

AE waveform recorder. Locations and crack types were assigned to individual AE events by applying moment tensor analysis [5] to the recorded waveforms; this is a method of quantitatively analyzing crack behavior by classifying cracks as tensile or shear and computing the probability of each crack type occurring. Young's modulus (JSCE-G502) and splitting tensile strength (JIS A 1113) were also determined in addition to the above measurements.

### 2-3 Experimental results and discussion

#### a) Mechanical properties of concrete

**Table 3** shows the mechanical properties of the tested concrete. The ratio of compressive strength ( $f'_c$ ) to tensile strength ( $f_t$ ) is expressed as the modulus of brittleness ( $f'_c/f_t$ ). It is known that when concrete, even lightweight concrete, is made extremely strong, tensile strength generally has a certain ceiling and does not continue to increase in proportion to the compressive strength [6]. This phenomenon was confirmed in this experiment, where the modulus of brittleness was about 12 for normal concrete but as high as 16 to 19 in the case of high-performance lightweight concrete. In observations of the crack surfaces after the compressive tests and splitting tensile strength tests, it was found that fracturing took place not only in the mortar but also within coarse aggregate particles in the lightweight concrete specimens. On the other hand, in normal concrete, fractures developed in the mortar and at the interface between mortar and coarse aggregate

particles. Comparing the two types of high-performance artificial lightweight aggregate HL12 (density: 1.2 g/cm<sup>3</sup>) and HL08 (density: 0.85 g/cm<sup>3</sup>), the compressive strength of the concrete was higher and the modulus of brittleness lower with the more dense aggregate. Close observation of the crack surfaces showed that almost 100% of coarse aggregate particles had fractured in concrete containing HL08, while about 40% remained intact in concrete containing HL12; in this case, cracks developed around, not through, the aggregate particles. This suggests that the brittleness modulus may be restrained by increasing the density, or strength, of the aggregate.

Young's modulus decreased with the lower density concrete mixture, although it is still a function of compressive strength and density in the case of high-performance lightweight concrete, just as in normal concrete.

b) Fracture process under compressive stress

**Figure 2** shows the frequency of AE activity under compressive stress. In the case of normal concrete, few AE events were detected until the stress level reached 80%, with the number of detected AE events rising very rapidly thereafter. On the contrary, in the lightweight concrete case, AE events began at an early stage and AE activity increased steadily as the stress increased. This suggests a clear difference in the cracking behavior of the two types of concrete.

Typically, the Young's modulus of aggregate is larger than that of the matrix in normal concrete. The opposite is true in lightweight concrete. It is accepted, therefore, that the distribution of stress in and around aggregate particles differs between normal concrete and lightweight concrete, as illustrated in **Figure 3** [7]. In order to determine whether, in the case of lightweight concrete under compressive stress, cracks predominate within the aggregate particles or in the mortar, moment tensor analysis was carried out using the measured AE waveforms. The authors adopted a method described by Ohtsu, et al. [8], who evaluated the probability of crack occurrence by classifying cracking into three categories depending on the proportion of shear mode cracks. Cracking is categorized as shear type when the shear mode accounts for over 60% of cracks, as mixed type when the shear mode is in the range 40%-60%, and as tensile type when the shear mode is below 40%. **Figure 4** shows crack modes and locations estimated by moment tensor analysis, and **Figure 5** shows occurrence rates for individual crack modes until fracture. According to these figures, shear mode cracks accounted for over 50% of the total until fracture in normal concrete; on the contrary, tensile mode cracks occurred in considerable numbers from an early stage and accounted for over 50% until fracture in lightweight concrete. Slightly more tensile mode cracks were observed in concrete with HL12 than in concrete with HL08. From these results of crack mode analysis and by observing damage to aggregate particles on the crack surface, it is found that as the density of the lightweight aggregate increases, the probability of tensile mode cracks occurring falls slightly. This suggests that the tensile mode cracks detected during the tests were tensile cracks in both aggregate particles and mortar.

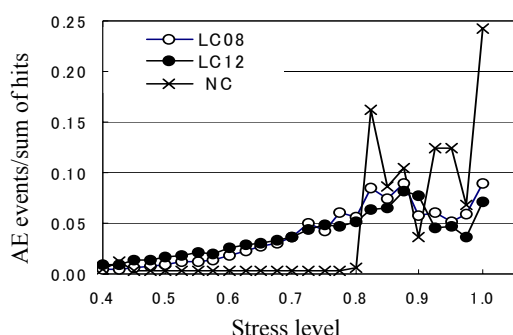


**Fig.2** AE event frequency

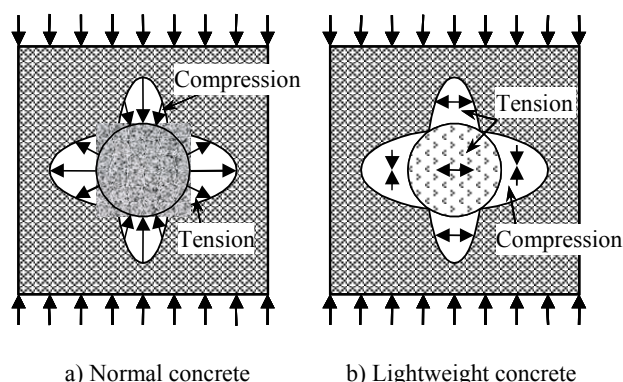


**Fig.3** Stress conditions in and around an aggregate

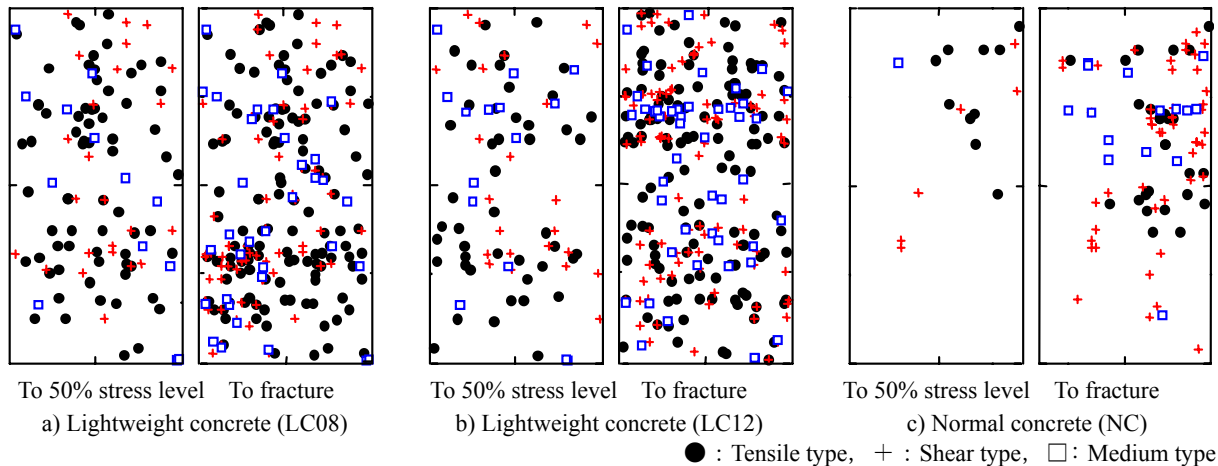


Fig.4 Moment tensor analysis results

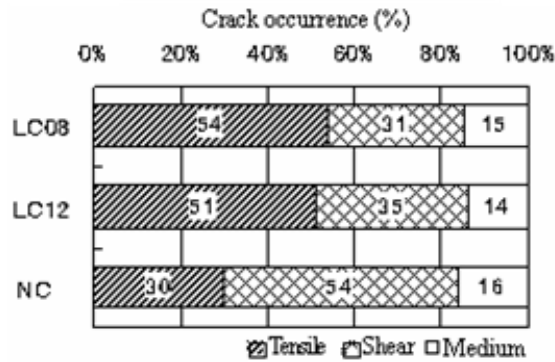


Fig.5 Occurrence of individual crack types (at fracture)

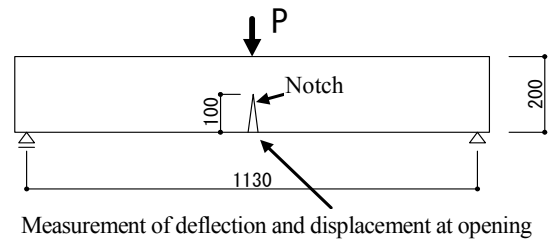


Fig.6 Applying load to specimen

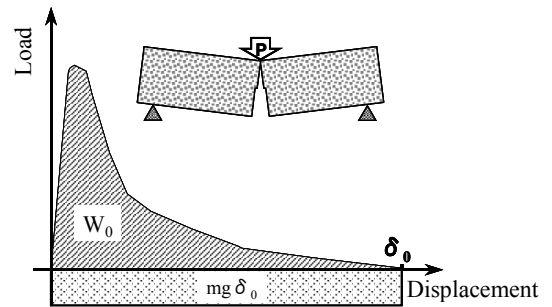


Fig.7 Determining fracture energy from load-displacement curve

### 3. FRACTURE PROCESS UNDER BENDING STRESS

#### 3-1 Experiment

Fracture energy was measured in accordance with the RILEM method “Determination of the Fracture Energy of Mortar and Concrete by Means of Three-point Bend Tests on Notched Beams” in order to investigate micro-crack behavior under bending stress in lightweight concrete containing high-performance artificial lightweight aggregate.

#### 3-2 Test method

Once again, the materials and mix proportions given in **Table 1** and **Table 2** were used. Beam specimens measuring 200 mm high  $\times$  100 mm wide  $\times$  1,200 mm long (**Figure 6**) were cured at  $20 \pm 2^\circ\text{C}$  and 90% relative humidity or above after demolding until immediately before testing. Before the loading test, a notch was formed at the center of each specimen to half the beam height (100 mm) with a diamond cutter (blade

thickness: 2 mm).

A three-point bending load was applied under displacement control using the test equipment (effective span: 1,130 mm), and measurements taken of deflection at the center of the span and displacement at the opening. AE activity was measured during loading in the same manner as in Section 2 above, using AE sensors attached around the notch opening.

Fracture energy, which is the energy per unit area required to generate cracks and is expressed by Eq. (1), was calculated from the area  $W_0$  below the load-displacement curve and corrected for the effect of specimen self weight as shown in **Figure 7**.

$$G_F = (W_0 + mg \cdot \delta_0) / A_{lig} \quad \text{Eq. (1)}$$

Where,  $G_F$ : fracture energy ( $J/m^2$ );  $W_0$ : area below the load-displacement curve (N·m);  $m$ : mass of effective span of the beam (kg);  $g$ : acceleration due to gravity ( $m/s^2$ );  $\delta_0$ : displacement in the beam at fracture (m); and  $A_{lig}$ : fractured area of the beam ( $m^2$ ).

Tension softening curves were estimated from the load-displacement relationships at opening, as obtained by poly-linear approximation [9], [10] using a finite element method incorporating a virtual crack model at the center of the specimen.

### 3-3 Experimental results and discussion

#### a) Fracture energy

**Table 4** shows the results of the fracture energy test. Lightweight concrete exhibited reduced displacement at fracture than normal concrete. Fracture energy, also, was lower by about 70%. Comparing the two types of high-performance artificial lightweight aggregate, displacement at fracture as well as fracture energy were slightly larger for the concrete containing HL12, which has a density of  $1.2 \text{ g/cm}^3$ , than for the concrete containing HL08 with a density of  $0.85 \text{ g/cm}^3$ .

The load-displacement curves in **Figure 8** show notable differences in behavior between normal and high-performance lightweight concretes in the downward region beyond the maximum stress.

**Figure 9** shows the locations and fracture modes of individual micro-cracks as determined by moment tensor analysis. In normal concrete, micro-cracks form a distribution from around the top end of the notch toward the top edge of the beam, extending both vertically and widthwise through the cross section. However, in the concrete containing high-performance artificial lightweight aggregate, different behavior is observed. Micro-cracks were concentrated only in the area immediately above and around the top end of the notch in the case of the low-density HL08, while they were distributed in the vertical direction in the case of the high-density HL12. It is thought that fracturing in the LC12 case, where cracks were distributed over a wider area than with LC08, was not as rapid; that is, LC12 exhibited a certain tenacity that resulted in greater fracture energy than LC08 (**Table 4**). These results suggest that micro-cracks in normal concrete disperse

**Table 4** Mechanical properties of concrete specimens

Symbol	Density (kg/l)	Compressive strength ( $N/mm^2$ )	Displacement at fracture (mm)	Fracture energy ( $J/m^2$ )
LC08	1.73	43.0	0.46	43.3
LC12	1.87	56.9	0.52	52.9
NC	2.38	42.5	1.41	163.9

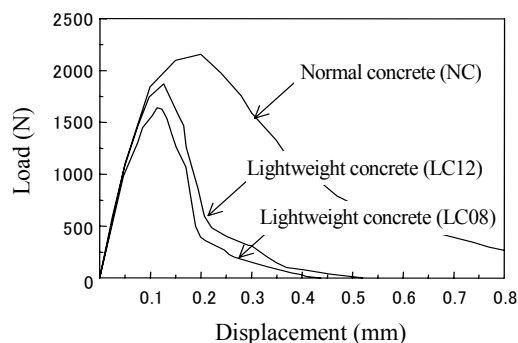


**Fig.8** Load-displacement curve

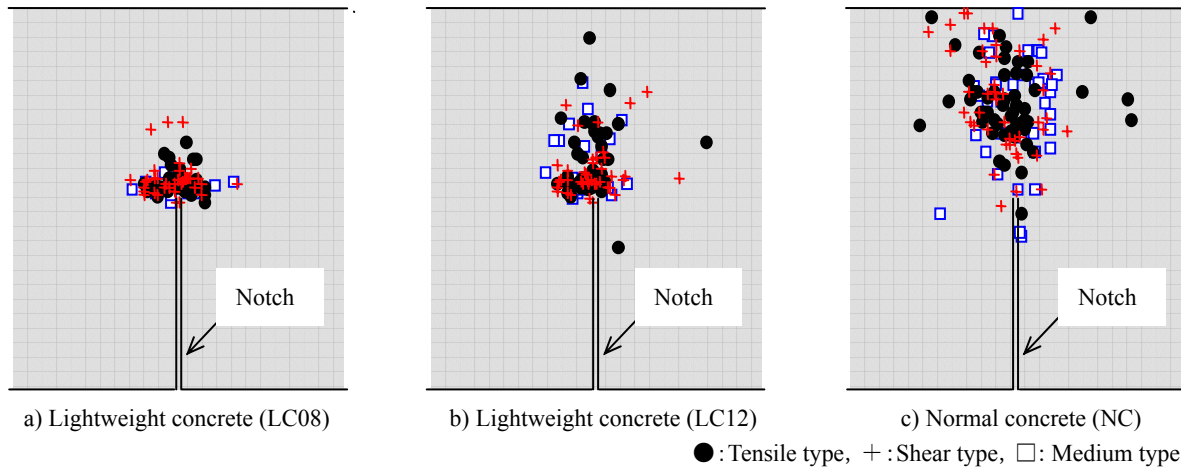


**Fig.9** Moment tensor analysis results

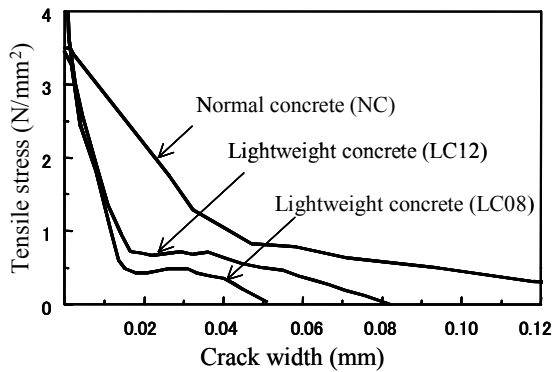


**Fig.10** Tension softening curve estimation results

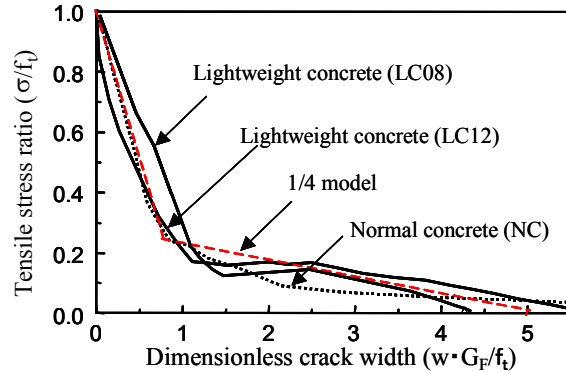


**Fig.11** Dimensionless tension softening curves

while avoiding the particles of coarse aggregate, while fracturing is immediate in concrete containing high-performance artificial lightweight aggregate because micro-cracks in aggregate particles and in the mortar instantly join together.

When normal concrete is subject to tensile stress, most micro-cracks occur in the mortar or at the interface between mortar and aggregate particles. As they lengthen, their paths avoid the particles of coarse aggregate. On the other hand, in lightweight concrete, the particles of coarse aggregate tend to split, so fractures spread through the aggregate and mortar together. The fracture energy of LC12 was slightly larger than that of LC08, probably because about 30% of coarse aggregate particles around the fracture surface were not affected by cracks as a result of the aggregate's higher strength.

#### b) Tension-softening characteristics

Tension softening curves obtained by multi-linear approximation (**Figure 10**) show that tension-softening behavior varies significantly with concrete type. The higher the density, or strength, of the aggregate, the tougher the concrete, and the curves slope more gently.

**Figure 11** shows dimensionless forms of the tension softening curves [11]. Although the fracture energy of high-performance lightweight concrete is lower than that of normal concrete, there is no significant difference in the ratio of first and second region gradients and for both types the curves are of similar shape (and are close to the 1/4 model).

## 4. INFLUENCE OF AGGREGATE QUALITY ON MECHANICAL PROPERTIES OF CONCRETE

### 4-1 Experiments

After examining the fracture behavior of high-performance lightweight concrete under compressive and bending stresses, as described in the previous sections, the authors studied the influence of aggregate quality on the mechanical properties of concrete. Strength and fracture energy tests were carried out using concrete containing various combinations of lightweight aggregate with different qualities and a matrix with different strengths. Experiments were carried out in three series', from I to III, using the materials shown in **Table 5**. Parameters were varied as shown in **Table 6**. Series I was designed to test the influence of type of coarse aggregate and strength of matrix. Series II was for the influence of the bulk volume of coarse aggregate per unit volume of concrete (the "unit volume of coarse aggregate"). Series III was for the influence of maximum size of coarse aggregate. Two types of normal concrete with different strengths and mortar matrices, achieved by wet screening, were also tested for the purpose of comparison.

### 4-2 Test method

**Table 7** shows mix proportions of concrete used for the experiments. The matrix strength was adjusted by replacing part of the cement with low-reactive, finely powdered limestone with a specific surface area of 4,000 cm<sup>2</sup>/g, thereby changing the water-cement ratio. The unit volume of coarse aggregate for Series I and III tests was 350 l/m<sup>3</sup>, and the maximum size of coarse aggregate for Series I and II tests was 15 mm. The addition of an AE superplasticizer and an AE agent was adjusted as required so as to yield a concrete slump of 8×2.5 cm and an air content of 5.5×1.5%.

**Table 5** Materials used in concrete

Material	Symbol	Description	Properties
Cement	C	Normal portland cement	Density: 3.16 g/cm <sup>3</sup> ; specific surface area: 3,350 cm <sup>2</sup> /g
Fine aggregate	S	River sand (Ogasa)	Density <sup>*1</sup> : 2.58 g/cm <sup>3</sup> ; water absorption: 1.19%
Coarse aggregate (G)	HL08	Perlite high-performance lightweight aggregate	Granulated type; density <sup>*1</sup> : 0.88 g/cm <sup>3</sup> ; 24-hour water absorption: 2.26%
	HL12	Perlite high-performance lightweight aggregate	Granulated type; density <sup>*1</sup> : 1.20 g/cm <sup>3</sup> ; 24-hour water absorption: 1.76%
	HL18	Fly ash high-performance lightweight aggregate	Granulated type; density <sup>*1</sup> : 1.8 g/cm <sup>3</sup> ; 24-hour water absorption: 2.42%
	AL12	Expanded shale conventional lightweight aggregate	Non-granulated type; density <sup>*1</sup> : 1.22g/cm <sup>3</sup> ; 24-hour water absorption: 34.2%
	CS26	Crushed stone #6 (Oume)	Density <sup>*1</sup> : 2.64 g/cm <sup>3</sup> ; water absorption: 0.67%
Admixture	B	Finely powdered limestone	Density: 2.70 g/cm <sup>3</sup> ; specific surface area: 4,000 cm <sup>2</sup> /g
	SP	AE superplasticizer	Polycarbonate type
	AE	AE agent	Modified alkylcarbonate type

\*1: oven-dry state

**Table 6** Experimental factors

Series	Factors	Description				
		1	2	3	4	5
I	A: Aggregate type	HL08	HL12	HL18	AL12	CS26
	B: Matrix strength (N/mm <sup>2</sup> )	15 (M15)	30 (M30)	45 (M45)	60 (M60)	75 (M75)
II	A: Unit volume of coarse aggregate (L/m <sup>3</sup> )	300 (Gv300)	350 (Gv350)	400 (Gv400)	—	—
	B: Matrix strength (N/mm <sup>2</sup> )	30 (M30)	60 (M60)	—	—	—
III	A: Maximum size of coarse aggregate (mm)	10 (Gs10)	15 (Gs15)	20 (Gs20)	—	—
	B: Matrix strength (N/mm <sup>2</sup> )	30 (M30)	60 (M60)	—	—	—

**Table 7** Concrete proportions

Series	Symbol	G type	G unit volume (m <sup>3</sup> /m <sup>3</sup> )	G max. size (mm)	Target matrix strength (N/mm <sup>2</sup> )	B ratio <sup>*1</sup> (vol.%)	W/C (%)	s/a (%)	Air (%)	Unit content (kg/m <sup>3</sup> )					Chemical admixture (C × %)		Density of concrete mixture (kg/m <sup>3</sup> )	
										W	C	B	S	G	SP	AE	Calculate d	Measure d
I	HL08M15	HL08	350	15	15	70	116.7	44.4	5.5	165	141	282	739	308	0.20	0.008	1642	1635
	HL08M30				30	55	77.8				212	222			0.25	0.005	1653	1610
	HL08M45				45	40	58.3				283	161			0.25	0.000	1663	1648
	HL08M60				60	20	43.8				377	81			0.35	0.000	1677	1661
	HL08M75				75	0	35.0				471	0			0.60	0.009	1690	1687
	HL12M15	HL12	350	15	15	70	116.7	44.4	5.5	165	141	282	739	419	0.25	0.008	1754	1751
	HL12M30				30	55	77.8				212	222			0.30	0.005	1765	1742
	HL12M45				45	40	58.3				283	161			0.30	0.005	1774	1753
	HL12M60				60	20	43.8				377	81			0.45	0.002	1788	1777
	HL12M75				75	0	35.0				471	0			0.55	0.002	1802	1798
	HL18M15	HL18	350	15	15	70	116.7	44.4	5.5	165	141	282	739	625	0.20	0.007	1968	1957
	HL18M30				30	55	77.8				212	222			0.20	0.005	1978	1972
	HL18M45				45	40	58.3				283	161			0.25	0.004	1988	1952
	HL18M60				60	20	43.8				377	81			0.40	0.001	2002	2004
	HL18M75				75	0	35.0				471	0			0.65	0.002	2016	2020
	AL12M15	AL12	350	15	15	70	116.7	44.4	5.5	165	141	282	739	427	0.10	0.008	1900	1929
	AL12M30				30	55	77.8				212	222			0.10	0.006	1911	1939
	AL12M45				45	40	58.3				283	161			0.20	0.003	1921	1926
	AL12M60				60	20	43.8				377	81			0.20	0.002	1935	1928
	AL12M75				75	0	35.0				471	0			0.45	0.001	1948	1930
II	Gv300M30	HL12	300	15	30	55	77.8	44.4	5.5	165	141	282	739	419	0.25	0.008	1820	1850
	Gv300M60				60	20	43.8				212	222			0.30	0.005	1846	1846
	Gv350M30	HL12	350	15	30	55	77.8	44.4	5.5	165	283	161	739	419	0.30	0.005	1765	1742
	Gv350M60				60	20	43.8				377	81			0.45	0.002	1788	1777
	Gv400M30	HL12	400	15	30	55	77.8	44.4	5.5	165	471	0	739	419	0.55	0.002	1716	1718
	Gv400M60				60	20	43.8				471	0			0.55	0.002	1738	1738
III	Gs10M30	HL12	350	10	30	55	77.8	44.4	5.5	165	141	282	739	419	0.25	0.008	1767	1778
	Gs10M60				60	20	43.8				212	222			0.30	0.005	1791	1798
	Gs15M30			15	30	55	77.8				283	161			0.30	0.005	1765	1742
	Gs15M60				60	20	43.8				377	81			0.45	0.002	1788	1777
	Gs20M30			20	30	55	77.8				471	0			0.55	0.002	1734	1777
	Gs20M60				60	20	43.8				471	0			0.55	0.002	1758	1762
Control	CS26M30	CS26	350	15	30	55	77.8	44.4	5.5	165	212	222	739	931	0.30	0.003	2269	2242
	CS26M60				60	20	43.8				377	81			0.45	0.001	2293	2264

\*1: replacement ratio of finely powdered limestone for cement

Cement, finely powdered limestone, fine aggregate, and coarse aggregate were dry mixed for 15 seconds, then water and chemical admixtures were added. All components were then mixed for a total of 2 minutes in a 30-l Omni Mixer. The fresh concrete was confirmed as satisfying the quality requirements using JIS test methods: JIS A 1101 for slump; JIS A 1116 for density and air content (mass method); and JIS A 1128 for air content (pressure method). The concrete containing HL12 was wet screened after mixing to obtain mortar specimens.

After demolding at the age of 1 day and curing underwater at 20°C until the age of 28 days, the specimens were tested for compressive strength (JIS A 1108), splitting tensile strength (JIS A 1113), flexural strength (JIS A 1106) and shear strength (JSCE-G533) [12].

Fracture energy was measured in accordance with the RILEM method “Determination of the Fracture Energy of Mortar and Concrete by Means of Three-point Bend Tests on Notched Beams”. Three specimens measuring 100×100×400 mm were prepared for each mix proportion, using the same curing and aging

conditions as in the strength tests. Notches were provided in the specimens by inserting a 50 mm high by 3 mm thick acrylic plate into the form. Loading was applied at a displacement rate of 0.1 mm per minute using displacement control loading equipment with an effective span of 300 mm, and deflection at the center of each specimen was measured using a laser displacement meter (resolution: 0.05  $\mu\text{m}$ ). Loading was measured using a load cell. Fracture energy was calculated using Eq. (1) in the same manner as in the previous experiments.

#### 4-3 Mechanical properties and discussion

##### a) Influence of aggregate and matrix strength

**Figure 12** shows the compressive, tensile, flexural, and shear strength of concrete specimens containing different types of lightweight aggregate with respect to the measured matrix strength. Concrete strength increased with an increase in matrix strength, but reached a certain ceiling at a certain higher matrix strength. Concrete strength also increased as aggregate density increased. The difference of concrete strength was more significant as the matrix strength increased. The difference between concrete strength and matrix strength was also remarkable when the aggregate density was low. The compressive strength of coarse aggregate particles was estimated using Bache's method [13] as shown in Eq. (2).

$$\sigma_c/\sigma_m = (\sigma_a/\sigma_m)^n \quad \text{Eq. (2)}$$

(but about  $2 < \sigma_m/\sigma_a < \text{about } 15$ , and  $0 < n < \text{about } 0.5$ )

Where,  $\sigma_a$ : strength of coarse aggregate particles;  $\sigma_m$ : compressive strength of matrix;  $\sigma_c$ : compressive strength of concrete; and  $n$ : ratio of coarse aggregate in concrete by absolute volume. Since Eq. (2) is an experimental equation in which the matrix strength is higher than two times the aggregate strength, estimates derived from measured values for specimens containing matrixes M60 and M70 give a coarse aggregate strength of 24.3  $\text{N/mm}^2$  for HL08, 32.1  $\text{N/mm}^2$  for AL12, 40.0  $\text{N/mm}^2$  for HL12, and 57.8  $\text{N/mm}^2$  for HL18. These results demonstrate that the lightweight aggregate strength influences the mechanical properties of the concrete.

**Figure 13** shows the relationship between aggregate strength as determined above and oven-dry particle density. According to this chart, comparing the two types of lightweight aggregate which has equal density, the strength of high-performance artificial lightweight aggregate (HL12) was about 8  $\text{N/mm}^2$  higher than that of conventional lightweight aggregate (AL12). This is probably due to the difference between voids in high-performance artificial lightweight aggregate and conventional lightweight aggregate; in the former, they are isolated whereas in the latter they are mostly continuous. This difference in void structure is also the cause of the difference in absorption ratio.

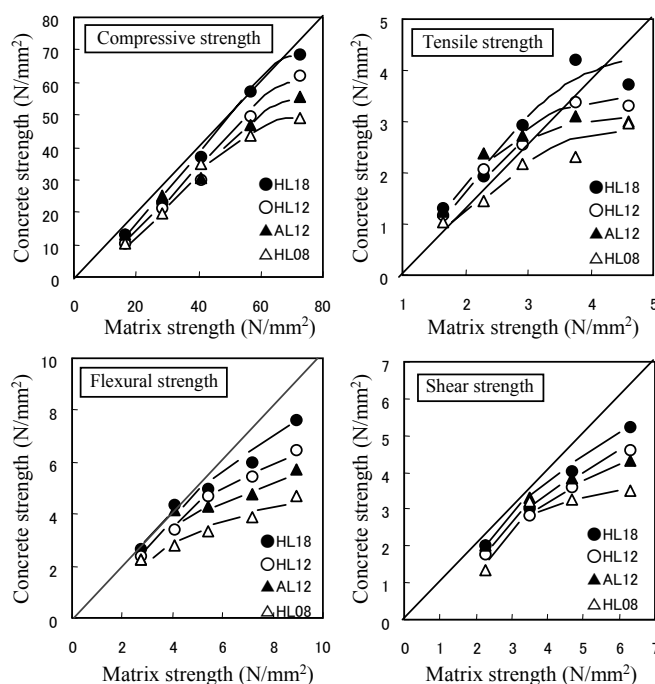


**Fig.12** Relationships between concrete strength and matrix strength

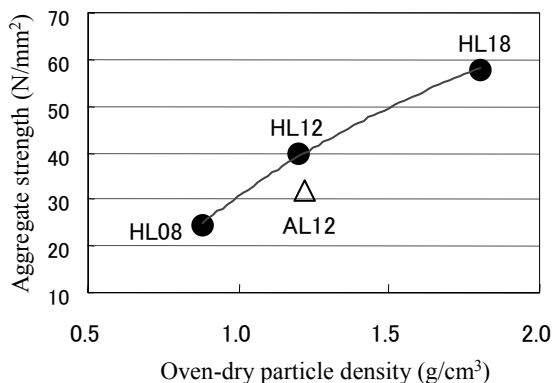


**Fig.13** Relationship between the aggregate strength and the oven-dry particle density

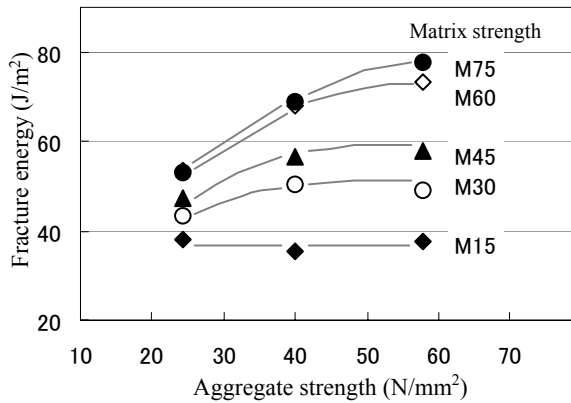


**Fig.14** Fracture energy against aggregate strength (with high performance lightweight aggregate)

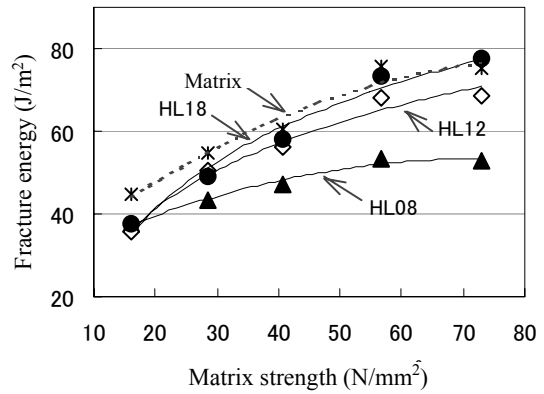


**Fig.15** Fracture energy against matrix strength (with high performance lightweight aggregate)

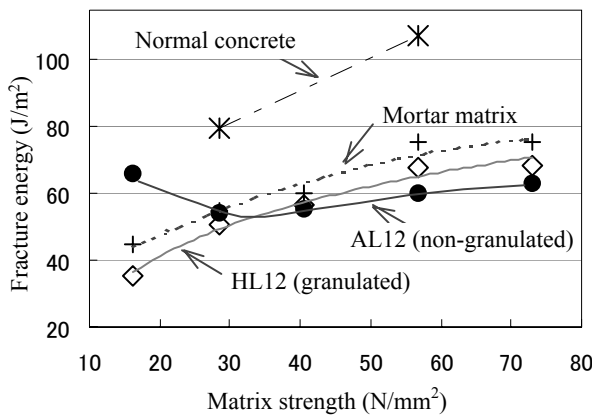


**Fig.16** Fracture energy against matrix strength (with different types of aggregate)

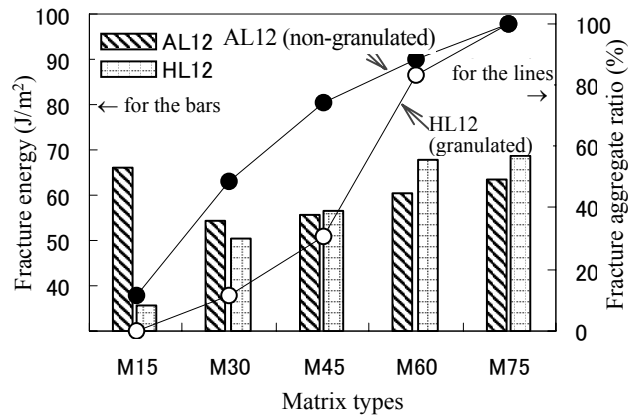


**Fig.17** Fracture aggregate ratio and fracture energy

**Figure 14** and **Figure 15** show the relationships between fracture energy of high-performance lightweight concrete and aggregate strength and matrix strength, respectively. Generally, the greater the aggregate strength, and the greater the matrix strength, then the higher the fracture energy of the lightweight concrete, as shown in **Figure 14**. However, with respect to the various combinations of aggregate and matrix strength, the influence of aggregate strength on fracture energy is small when the matrix strength is low, whereas it is greater as the matrix strength increases. This means that the concrete fracture energy is significantly influenced by the combination of aggregate and matrix strength. It can be seen from **Figure 15** that although the concrete fracture energy reached a certain ceiling as the matrix strength increased, the higher the aggregate strength, the higher this ceiling.

**Figure 16** compares high-performance lightweight concrete (with HL12), concrete containing conventional lightweight aggregate, normal concrete, and the mortar matrix alone. The fracture energy of high-performance lightweight concrete is almost equivalent to that of the mortar matrix, while that of normal concrete is up to 1.5 to 2 times greater. Compared with concrete containing conventional lightweight aggregate AL12, high-performance lightweight concrete exhibits higher fracture energy when a high-strength matrix of 40 N/mm<sup>2</sup> or above is used. On the other hand, the fracture energy is higher for concrete containing conventional lightweight aggregate when a low-strength matrix of 30 N/mm<sup>2</sup> or below is used. **Figure 17** shows fracture energy (bar graphs) and fractured aggregate ratio (line graphs) for concrete containing high-performance artificial lightweight aggregate and conventional lightweight aggregate of equal density. The fractured aggregate ratio is the ratio of the number of fractured coarse aggregate particles to the sum of all coarse aggregate particles present at the crack surface. According to these graphs, the smaller the fracture aggregate ratio, the higher the fracture energy of AL12. It is thought that when the coarse aggregate is stronger than the matrix and has an irregular shape, as in the case of AL12, cracks develop around the aggregate particles, and the engagement of aggregate particles at the crack surface provides

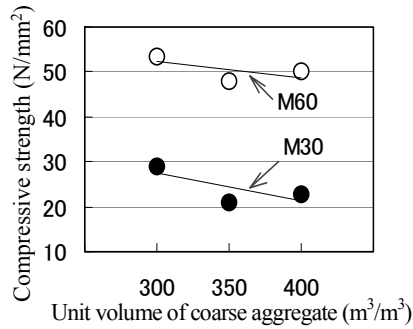


**Fig.18** Compressive strength against unit volume of coarse aggregate

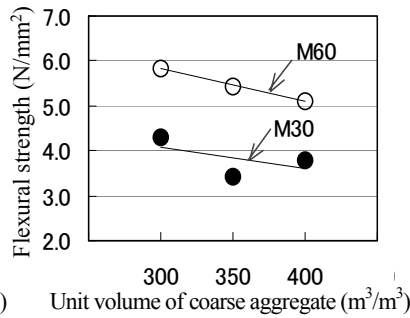


**Fig.19** Flexural strength against unit volume of coarse aggregate

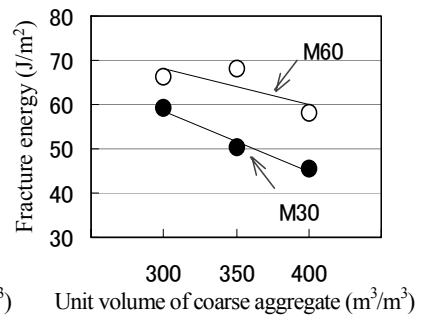


**Fig.20** Fracture energy against unit volume of coarse aggregate

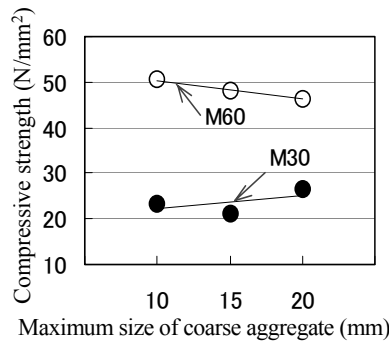


**Fig.21** Compressive strength against maximum size of coarse aggregate

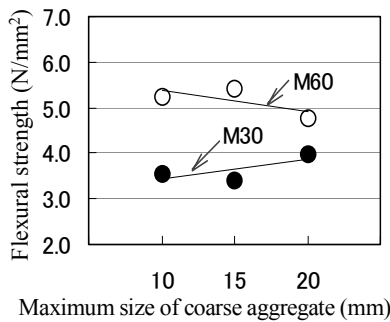


**Fig.22** Flexural strength against maximum size of coarse aggregate

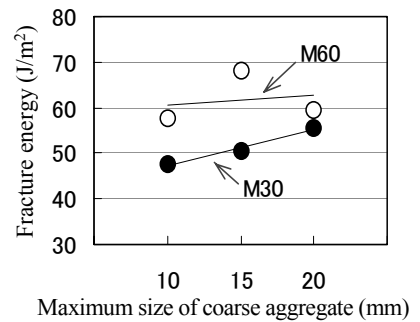


**Fig.23** Fracture energy against maximum size of coarse aggregate

further resistance to crack extension, thereby enhancing the fracture energy of the concrete.

b) Influence of coarse aggregate content and maximum size

The experimental results for the Series II tests are shown in **Figure 18** to **Figure 20** as relationships between unit volume of coarse aggregate and compressive strength, flexural strength, and fracture energy. The higher the coarse aggregate content, the lower these characteristic values for the concrete. With regard to fracture energy in particular, the influence of coarse aggregate content is more significant than on the strength values. All characteristic values increase with rising mortar matrix strength, no variation in this tendency is seen with different matrix strengths within the range of this experiment.

The experimental results for the Series III tests are shown in **Figure 21** to **Figure 23** as relationships between maximum coarse aggregate size and compressive strength, flexural strength, and fracture energy. In normal concrete with a constant water-cement ratio, concrete strength tends to decrease as the coarse aggregate size increases [14]. In high-performance lightweight concrete, however, this trend is hardly noticeable at high matrix strengths (M60) and is even slightly reversed when the matrix strength is low (M30). With the low-strength matrix, the larger the maximum coarse aggregate size, the higher the characteristic values of the concrete, with a particularly significant influence on the fracture energy (as seen in the influence of coarse aggregate content in Series II). More cracks tend to avoid the aggregate particles when the matrix strength is lower, so cracks must travel longer distances to circumvent the aggregate particles as they become larger. This results in enhanced fracture energy [15].

**Figure 24** shows a conceptual outline of the relationship between lightweight concrete fracture energy and matrix strength, providing a qualitative summary of the influence of individual factors on fracture energy. In the region where the coarse aggregate strength exceeds matrix strength ( $\sigma_a > \sigma_m$ ), the fracture energy is highly prone to the influence of aggregate configuration factors, such as the shape and size of the coarse aggregate particles, since cracks tend to avoid the coarse aggregate particles as they lengthen. The fracture energy is higher when aggregate particles are irregular in shape, because the engagement of coarse aggregate particles is improved and cracks must travel longer distances to avoid the particles. A larger aggregate size also increases the fracture energy due to the increased crack path. On the contrary, in the region where the matrix

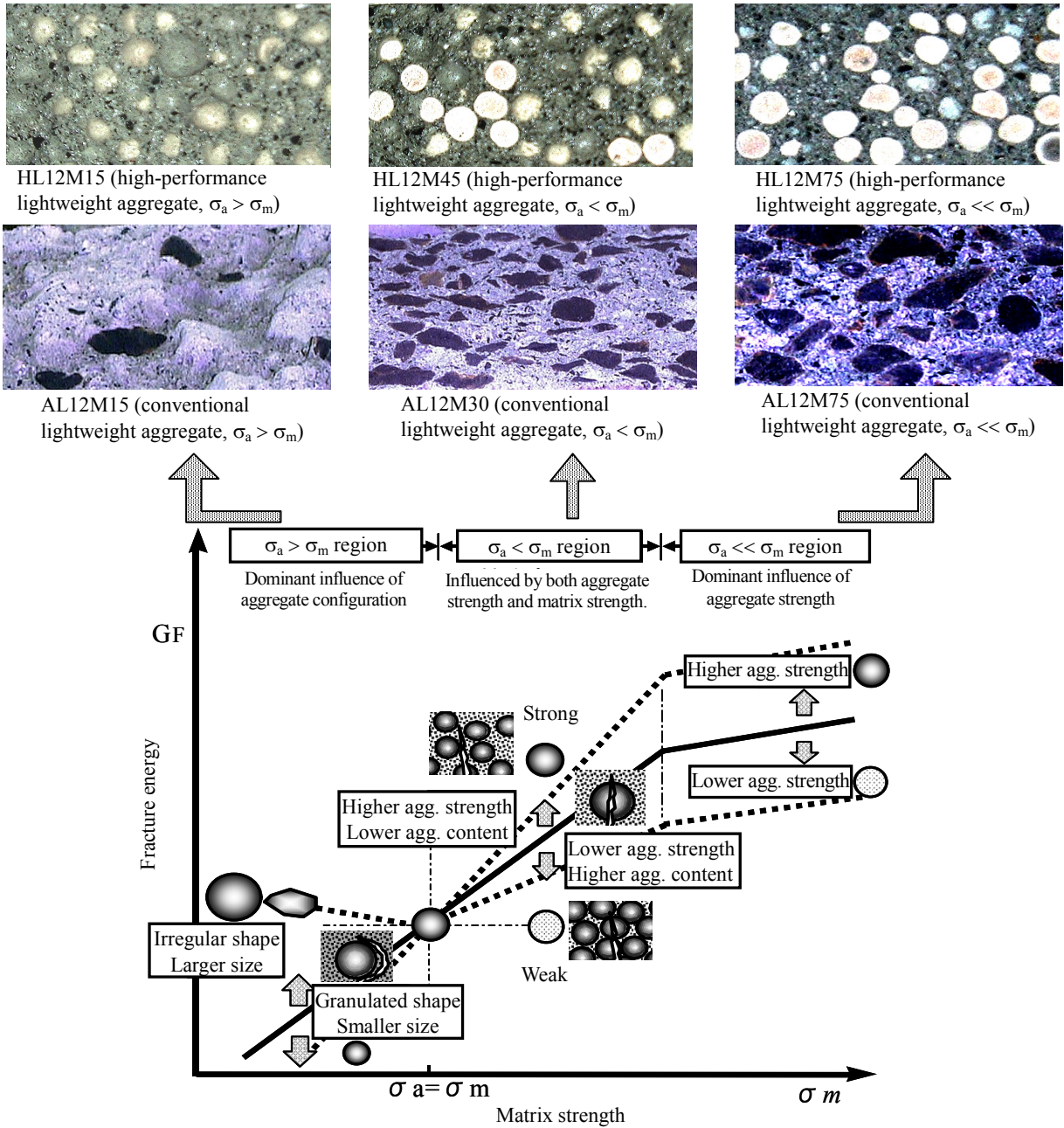


Fig.24 Factors influencing fracture energy of concrete

strength is predominant ( $\sigma_a < \sigma_m$ ), both the aggregate strength and the matrix strength influence the fracture energy, since cracks pass through the coarse aggregate particles. The content of aggregate also has an influence in this region because of the lower strength of the lightweight aggregate. The greater the unit volume of coarse aggregate, the smaller the fracture energy. If matrix strength is much greater than that of the coarse aggregate ( $\sigma_a \ll \sigma_m$ ; where the matrix strength is over 1.5 to 2 times the aggregate strength within the range tested in this experiment), the fracture energy reaches a certain ceiling even when a matrix with greater strength is used. This suggests that the fracture energy is influenced primarily by the aggregate strength in this region.

## 5. CONCLUSION

With the aim of quantitatively evaluating the fracture characteristics of high-performance lightweight

concrete (containing ordinary fine aggregate and high-performance artificial lightweight coarse aggregate), AE techniques were used to observe the energy released during unconfined compressive and flexural fracture tests. Strength and fracture energy tests were also carried out on concrete specimens made with lightweight coarse aggregate of different qualities and matrices of different strengths to clarify the influence of aggregate quality on the mechanical properties of concrete. The results obtained during this study are summarized below.

(1) Under compressive stress, concrete containing high-performance artificial lightweight aggregate exhibits different stress behavior to normal concrete, both in the aggregate and in the surrounding matrix. Tensile-mode micro-cracks occur within the aggregate even when the stress is still low, and these connect with cracks in the mortar to form a continuous crack, resulting in concrete fracture accompanied by fracture of the aggregate particles.

(2) Under bending stress, the occurrence of micro-cracks in concrete containing high-performance artificial lightweight aggregate is concentrated in the region immediately above a notch, and cracks in the aggregate and mortar join rapidly together, resulting in fracture of the concrete accompanied by fracture of the aggregate particles.

(3) Although the fracture energy of concrete containing high-performance artificial lightweight aggregate is lower than that of normal concrete, fracture characteristics can be improved by using aggregate of greater strength.

(4) The strength of high-performance artificial lightweight aggregate, which contains many isolated voids, is proportional to the aggregate density, and this relation holds at higher strength levels than in the case of conventional lightweight aggregate.

(5) The fracture energy of concrete containing lightweight coarse aggregate is influenced by the coarse aggregate strength, the matrix strength, and the unit volume and size of the coarse aggregate; further, the influence of each characteristic varies with the ratio of coarse aggregate strength to mortar matrix strength.

(6) In the region where the strength of the coarse aggregate is greater than the matrix strength, aggregate configuration factors (such as coarse aggregate shape and size) influence the fracture energy significantly and cracks are confined mostly to the matrix. In particular, when the aggregate particles have irregular shape, the effects of particle engagement and the routing of cracks around the circumference of the particles both increase, so the fracture energy is greater. Larger aggregate sizes also enhance the fracture energy, since the length of cracks circumventing the particles increases.

(7) In the region where matrix strength is slightly greater than coarse aggregate strength, both aggregate strength and matrix strength influence the fracture energy, because cracks develop through the coarse aggregate particles. Since the strength of the lightweight aggregate is lower than that of the matrix, the higher the unit volume of coarse aggregate, the lower the fracture energy.

(8) In the region where the matrix strength is significantly higher than the strength of the coarse aggregate, the fracture energy reaches a certain ceiling when the matrix strength reaches a higher level. The fracture energy is influenced primarily by aggregate strength in this region.

## References

- [1]Okamoto, T., Ishikawa, Y., Tochigi, T., and Sasajima, M.: High-Performance Lightweight Concrete, Concrete Journal, JCI, Vol. 37, No. 4, pp. 12–18, 1999
- [2]Sone, T.: High-Strength Artificial Aggregate Using Coal-Ash as Raw Material, Concrete Journal, JCI, Vol. 36, No. 12, pp. 3–10, 1998
- [3]Shibata, T., Ishikawa, Y., Arai, R. and Okamoto, T.: A Study on Fracture Behavior and Microcrack Propagation of Concrete Using High-Performance Lightweight Aggregate, Proceedings of JCI, Vol.21, No.2, pp.913-918, 1999.6
- [4]Mori, D., Ishikawa, Y., Kokubu, K., Arai, R., and Okamoto, T.: Fracture Energy of Concrete Using High-Performance Lightweight Aggregate, Symposium on Diversification of Performance and Spreading of

Use of Lightweight Concrete, JCI, pp.11-16, 2000.8

[5]Ohtsu, M.: Theory and Characteristics of Acoustic Emission, Morikita Publishing, 1988

[6]Nishioka, S., Eguchi, I., and Kunimoto, K.: Studies on Concrete using Lightweight Aggregate, Cement and Concrete Research, No. 18, pp. 478–486, 1964

[7]Okada, K.: Advanced Concrete Engineering, Ohmsha, 1986

[8]Ohtsu, M.: Simplified Moment Tensor Analysis and Unified Decomposition of Acoustic Emission Source, Journal of Geophysical Research, 96(B4), pp. 6211–6221, 1991

[9]Kitsutaka, Y., Kamimura, K., and Nakamura, N.: Poly-Linear Approximation Analysis of Tension-Softening Diagram for Concrete, Journal of Structural and Construction Engineering, AIJ, No. 453, pp. 15–25, 1993

[10]Kurihara, N., Ando, T., Kunieda, M., Uchida, Y., and Rokugo, K.: Determination of Tension Softening Diagram of Concrete by Poly-Linear Approximation Analysis and Flexural Failure Behavior of Fiber Reinforced Concrete, Journal of JSCE, Vol. 30, No. 532, pp. 119–129, 1996

[11]Size Effect Subcommittee of JSCE Concrete Committee: Size Effect and Tension-Softening Diagram of Concrete Structures, Concrete Engineering Series No. 18, JSCE, 1997

[12]Japan Society of Civil Engineers: Standard Specification for Concrete Structure-2002, Test Methods and Specifications, Test Methods for Shear Strength of Steel Fiber Reinforced Concrete, pp. 220–221, 2002

[13]Ramos, C., and Shah, S. P.: Strength of Lightweight Aggregate and Concrete, Journal of Materials, Vol. 7, No. 3, pp. 380–387, 1972

[14]Cordon, W. A., and Gillespie, H. A.: Variables in Concrete Aggregates and Portland Cement Paste which Influence the Strength of Concrete, ACI Journal, Vol. 60, No. 8, pp. 1029–1050, 1963

[15]Nomura, N., Mihashi, H., and Niiseki, S.: Influence of Coarse Aggregate Size on Fracture Energy and Tension Softening of Concrete, Concrete Research and Technology, JCI, Vol. 2, No. 1, pp. 57–66, 1991